

Radiolysis of Electrolytes in Batteries: A Quick and Efficient Screening Process for the Selection of Electrolyte-Additive Formulations

Yanis Levieux-Souid, Jean-frédéric Martin, Philippe Moreau, Nathalie Herlin-Boime, Sophie Le Caër

▶ **To cite this version:**

Yanis Levieux-Souid, Jean-frédéric Martin, Philippe Moreau, Nathalie Herlin-Boime, Sophie Le Caër. Radiolysis of Electrolytes in Batteries: A Quick and Efficient Screening Process for the Selection of Electrolyte-Additive Formulations. Small Methods, 2022, 6 (10), pp.2200712. 10.1002/smtd.202200712 . cea-03760319

HAL Id: cea-03760319
https://cea.hal.science/cea-03760319

Submitted on 25 Aug 2022

HAL is a multi-disciplinary open access archive for the deposit and dissemination of scientific research documents, whether they are published or not. The documents may come from teaching and research institutions in France or abroad, or from public or private research centers.

L'archive ouverte pluridisciplinaire **HAL**, est destinée au dépôt et à la diffusion de documents scientifiques de niveau recherche, publiés ou non, émanant des établissements d'enseignement et de recherche français ou étrangers, des laboratoires publics ou privés.

Check for updates

small methods
www.small-methods.com

Radiolysis of Electrolytes in Batteries: A Quick and Efficient Screening Process for the Selection of Electrolyte-Additive Formulations

*Yanis Levieux-Souid, Jean-Frédéric Martin, Philippe Moreau, Nathalie Herlin-Boime, and Sophie Le Caër**

Understanding aging phenomena in batteries is crucial to the design of efficient, safe, and reliable energy storage devices as a part of the current green energy transition. Among the different aspects of a battery, the behavior of the electrolyte is a key parameter. Therefore, screening the aging characteristics of different electrolytes is of major interest. However, few screening studies exist because these are time-consuming and require the monitoring of numerous charge and discharge cycles. It has been demonstrated here that radiation chemistry, i.e., the interaction between ionizing radiation and matter, is a valuable tool to screen the behavior of various electrolytes within a few hours. Indeed, the rapid radiolysis of electrolytes leads to the production of the same gases as produced by electrochemical cycling (i.e., H_2, CO_2), and the ranking of electrolytes by their H_2 production yields similar performance ratings to those reported in the literature. Therefore, this direct comparison of electrolytes alone, lasting a few hours without any manufacturing operations such as the fabrication of electrochemical cells, demonstrates that controlled irradiation makes it possible to predict battery cycling behavior. Additionally, mechanisms involved in the degradation processes of different electrolytes are proposed.

1. Introduction

In the context of the energy transition, lithium-ion batteries (LIBs) are of great interest due to their efficiency as energy storage devices.[1–5] They exhibit very high gravimetric and volumetric energy densities and are used for various applications, such as in mobile microelectronics (e.g., mobile phones, laptop computers). More recently, high-energy density LIBs have also been considered as a power source for electric vehicles.[6,7] All batteries, however, show a decrease in their performance with increasing use.[8] The long-term stability of batteries is thus critical for the development of safe and reliable storage systems. In this context, the knowledge of aging phenomena during cycling, which are numerous, complex, and interrelated,[8] is essential.

Recent studies have shown that the performance and the reliability of batteries are strongly dependent on the choice of the electrolyte and can be improved by adapting its formulation.[9–17] The most commonly used electrolyte is presently composed of a mixture of cyclic and linear liquid carbonates containing a dissolved lithium salt, typically lithium hexafluorophosphate. This combination enables optimizing both the viscosity, which should be low and the dielectric constant, which should be high enough for ion transport.[9,18] However, since the electrolytes used in LIBs are not stable at the working potential of Li-ion anode materials, the electrolyte decomposes at the anode surface. This produces a solid-electrolyte interphase (SEI), which is of crucial importance to device performance and safety.[19–22]

In order to fulfill all requirements (e.g., good ion transport properties, good quality SEI, safety, performance), additives are typically introduced into the electrolyte solution in amounts lower than 10% by mass,[23] and many molecules can be used as additives.[23] This number of parameters and potential additive combinations leads to a high number of possible electrolyte formulations, and thus, there is a need for screening to identify the most efficient ones. However, screening so many formulations is a time-consuming task that requires many independent experiments and the construction and cycling of numerous electrochemical cells. For this reason, the comparison of electrolytes has mostly been assessed through computational studies[24–27]

Y. Levieux-Souid, N. Herlin-Boime, S. Le Caër
CEA/Saclay
DRF/IRAMIS/NIMBE UMR 3685, Bâtiment 546,
Gif-sur-Yvette Cedex F-91191, France
E-mail: sophie.le-caer@cea.fr

J.-F. Martin
CEA
LITEN
DEHT
STB
LM
Grenoble Cedex 9, F-38054, France

P. Moreau
Nantes Université
CNRS
Institut des Matériaux de Nantes Jean Rouxel
IMN
Nantes F-44000, France

The ORCID identification number(s) for the author(s) of this article can be found under https://doi.org/10.1002/smtd.202200712.

© 2022 The Authors. Small Methods published by Wiley-VCH GmbH. This is an open access article under the terms of the Creative Commons Attribution License, which permits use, distribution and reproduction in any medium, provided the original work is properly cited.

DOI: 10.1002/smtd.202200712

and very few experimental screening studies of electrolytes are found in the literature,[28,29] despite their major interest and significance. A recent study by Hildenbrand et al.[30] used a Bayesian-optimization algorithm but had to limit itself to mixtures of two carbonates probably because of extensive statistics involving long term cycling. In fact, the pioneering and comprehensive experimental work performed by J. R. Dahn's group (Figure S1, Supporting Information) is still the gold-standard for screening electrolytes for Li-ion batteries.[28] Over the years, the same group has continuously been adding more data on other systems till recently and based on similar protocols to that developed in 2014.[31] In the work performed in 2014,[28] the relationship between the nature and amount of several additives and the electrochemical performance of the formulation was determined by high precision coulometry and impedance spectroscopy in $LiCoO_2$/graphite pouch cells. The authors ranked additives and identified the best ones based on a marker representing the degradation of the battery, i.e., the charge slippage. The charge slippage is related to the production of gases, the degradation or evolution of the SEI, and its resistance, and is a good indicator of battery degradation since the main degradation phenomena were related to reduction processes that occured on graphite electrodes (silicon electrodes could also be considered).[28] Therefore, for comparison, reduction processes are targeted in our work.

It was recently demonstrated by our group that radiolysis, i.e., reactivity induced by the interaction between matter and ionizing radiation, is a powerful tool for the rapid identification of degradation products formed during battery cycling.[32,33] In other words, the reactive species formed in the irradiated solution are the same as those obtained during the charging of a battery.[33,34] This technique, therefore, makes it possible to mimic aging under electrolysis, but on much shorter time scales (of the order of a few minutes to a few hours) as compared to the much longer time scales of the electrochemical aging of batteries (ranging from a few weeks to several months). Moreover, pulsed radiolysis enables the performance of time-resolved experiments and is a very convenient tool to measure chemical rate constants and propose reaction mechanisms.[33–37]

The purpose of the present work is to i) demonstrate the use of radiolysis as an efficient technique to screen very quickly (in a few hours) various electrolytes; ii) check if the trends observed during battery cycling can be reproduced without the delicate protocol developed by Dahn's group and the necessity of reproducible electrochemical cell manufacturing. The search of a parameter able to achieve fast conclusions without battery cycling is a novel approach developed in the present paper. Lastly, iii) we propose degradation reaction mechanisms and discuss the effect of the presence of various additives in the mixtures.

2. Results and Discussion

Radiolysis experiments on different electrolytes and additives were carried out with a commercial gamma irradiator. The dose rate (4.7 ± 0.2 Gy min^{-1}, with 1 Gray, denoted Gy, equal to 1 J kg^{-1}) was measured using the Fricke dosimeter.[38] After each irradiation, gas measurements were performed by micro-gas chromatography (μ-GC) in order to identify and quantify the various gases produced. The reference electrolyte, i.e., containing no additives, used for these experiments was the same mixture used in the study by Dahn and coworkers,[28] namely 1 M $LiPF_6$ in ethylene carbonate (EC)/ethyl methyl carbonate (EMC) (3/7 v/v). The solvents and additives used in this study are displayed in **Figure 1**. Unless otherwise specified, the water content was never higher than 30 ppm.

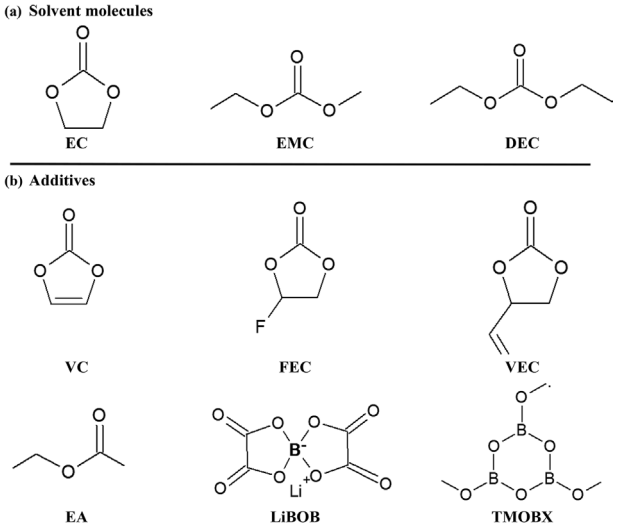


Figure 1. Chemical formulas of the a) solvents and b) additives used in the present work. The solvents are ethylene carbonate (EC), ethyl methyl carbonate (EMC), and diethyl carbonate (DEC). The additives are vinylene carbonate (VC), fluoroethylene carbonate (FEC), vinyl ethylene carbonate (VEC), ethyl acetate (EA), lithium bis(oxalate)borate (LiBOB), and trimethoxyboroxine (TMOBX). Salt is always lithium hexafluorophosphate at one molar concentration.

2.1. Quantification of H_2, CO, CO_2, and CH_4 Gas Production upon Irradiation

It is well-known that when using DEC or DEC/1 M $LiPF_6$, the production of H_2, CO, CO_2, and CH_4 is dominant compared to other gases (≈60%–65% of the total gas production).[32,33] The contribution of these four gases to the total gas production is expected to be even higher in the case of a cyclic carbonate.[34] Therefore, the present study based on EC and EMC electrolytes mainly concentrated on the production of these gases. The gas production under irradiation is presented in terms of radiolytic yield (i.e., the amount of gas produced per amount of energy deposited in the matter) in **Table 1** and Figures S2 and S3, Supporting Information. Typical data obtained with different additives are presented in Figure S2, Supporting Information. The amount of each gas increased linearly with the dose. The radiolytic yield was then obtained from the slope of the corresponding line (Figure S2, Supporting Information).

These measurements were systematically performed for the four gases and for each electrolyte under study. All experiments were performed in duplicate (or higher replication) to ensure reproducibility and to provide accurate radiolytic yield values. Importantly, the gases measured here (H_2, CO, CO_2, and CH_4) were already shown to form during the charging step of batteries using EC/EMC (1/1)/$LiPF_6$ 1 M as the electrolyte.[39] Both

© 2022 The Authors. Small Methods published by Wiley-VCH GmbH

Table 1. Radiolytic yields G [μmol J^{-1}] of the four main decomposition gases determined by μ-GC. The uncertainty is estimated to be 7%. The control electrolyte is EC/EMC (3/7 v/v) with 1 M $LiPF_6$.

	H_2	CH_4	CO	CO_2	Total
Control	0.079	0.039	0.074	0.312	0.504
+ 6% FEC	0.069	0.033	0.080	0.320	0.502
+ 4% FEC	0.070	0.035	0.073	0.449	0.627
+ 6% VC	0.048	0.023	0.093	0.327	0.491
+ 4% VC	0.049	0.021	0.102	0.302	0.474
+ 1% VC	0.051	0.027	0.076	0.307	0.461
+ 6% VEC	0.038	<0.01	0.065	0.399	0.512
+ 4% VEC	0.043	0.010	0.072	0.386	0.511
+ 6% LiBOB	0.062	0.024	0.083	0.258	0.427
+ 2% FEC + 2% VC	0.048	0.019	0.061	0.297	0.425
+ 2% FEC + 2% VEC	0.041	0.012	0.068	0.417	0.538
+ 2% VC + 2% VEC	0.041	0.011	0.086	0.422	0.560
+ 0.53% TMOBX	0.077	0.042	0.082	0.370	0.571
+ 0.3% TMOBX	0.082	0.047	0.089	0.338	0.556
+ 1% LiBOB + 6% VC	0.044	0.018	0.095	0.311	0.468
+ 6% EA	0.074	0.041	0.073	0.304	0.492

Table 1 and Figure S3, Supporting Information, show that the total amount of the four gases measured is not very sensitive to the nature of the additive. The total radiolytic yield was quite stable in the 4×10^{-7} to 6×10^{-7} mol J^{-1} range. It is also clear that among the four gases investigated, CO_2 was the most produced, with a radiolytic yield generally in the 3×10^{-7} to 4×10^{-7} mol J^{-1} range. H_2 and CO were formed in similar amounts, and CH_4 was generated to a lower extent.

Previous studies have shown that CO_2 is the most abundant gas produced after irradiation of DEC/$LiPF_6$ (1 M)[33] (linear carbonate) and PC (propylene carbonate, a cyclic carbonate)/$LiPF_6$ (1 M).[34] In fact, the differences between irradiated linear carbonates and cyclic carbonates were found in CO and H_2 production: cyclic carbonates produce clearly more CO than H_2, while it is the opposite for linear carbonates.[33–34] Our mixture of linear (EMC) and cyclic (EC) carbonates (as in the study of Dahn and coworkers) leads quite expectedly to compensation of these effects, i.e., CO and H_2 productions are rather similar (Table 1).

Conversely, one may wonder if one gas in particular could be correlated to the observed aging phenomena in cycling batteries and thus serve as a good indicator. From Table 1, we extracted the H_2 radiolytic yield as a function of the nature and the amount of the additive (**Figure 2**). For the sake of clarity and easier comparison, we used in Figure 2 the same color code as in the study by Dahn and coworkers (Figure S1, Supporting Information).[28] The behavior of the electrolyte containing an additive (EA) not studied by Dahn and coworkers[28] is represented in Figure 2 with an orange color.

Quite clearly, a large variation of the H_2 radiolytic yields as a function of the nature and the amount of the additive is obtained in Figure 2. While TMOBX and EA lead to H_2 yields similar to the control experiment, in all other cases, the presence of an additive tends to decrease the H_2 radiolytic yield. This trend

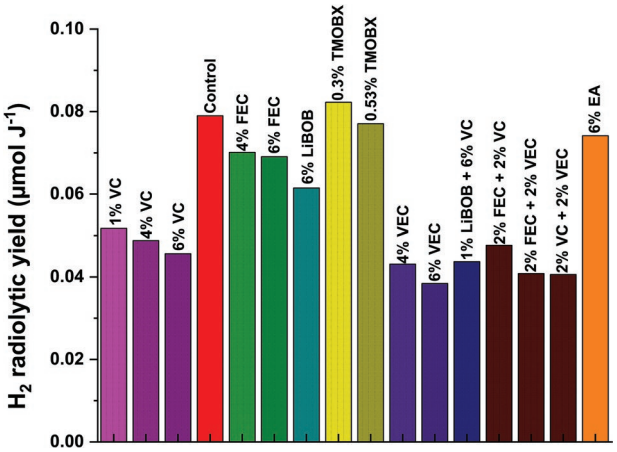


Figure 2. Evolution of the H_2 radiolytic yield, expressed in μmol J^{-1}, as a function of the amount (by mass) and the nature of the additive in the electrolyte. The reference electrolyte consists of EC/EMC (3/7 v/v) with 1 M of $LiPF_6$. For the purpose of comparison, the color code is the same as that used in Dahn and coworkers.[28] Another additive (not studied in reference[28]) was also investigated in the present work (EA). It is displayed on the right-hand side part of the figure with an orange color.

becomes even clearer as the concentration of additive increases (see for example VC and VEC cases in Figure 2). Interestingly, VC is known to decrease the H_2 production in lithium-ion batteries.[40,41] Indeed, the study by Bernhard et al. revealed that a cell made with a pre-formed VC-derived SEI on the graphite electrode leads to lower H_2 production.[40] Metzger et al. confirmed that the addition of VC allows the formation of a stable SEI and leads to lower H_2 production.[41]

Figure 2 shows clearly that VC and VEC are the most efficient additives for decreasing the H_2 radiolytic yield even when they are present in low amounts. Both compounds possess a carbon-carbon double bond (see Scheme 1). This suggests that this double bond reacts with a precursor of dihydrogen, such as the hydrogen atom, and forms a radical species, thus lowering the H_2 production.[42]

The H_2 radiolytic yields provides a way to classify the different additives. The following order is obtained from the radiolysis experiments (Figure 2): a mixture of two additives among FEC, VC and VEC < LiBOB with VC, VEC ≈ (similar to) VC < LiBOB < FEC < Control < TMOBX.

In the case of electrochemical experiments, the charge slippage, i.e., the decreasing performance of the battery due to unbalanced electrochemical reactions of positive versus negative materials, is correlated to several aging mechanisms including gas production, the SEI degradation or evolution, and its impedance. In the experiments performed by Dahn and coworkers (Figure S1, Supporting Information), the following order, according to charge slippage, was obtained:[28] mixture of two additives among FEC, VC and VEC < LiBOB with VC ≈ VC < LiBOB ~ FEC < Control < TMOBX.

We excluded here the results obtained with VEC by Dahn and coworkers from this order, as the experiment performed with 6% VEC exhibited a particularly large error bar, attributed to a large amount of gas formed during the cycling.[28]

Therefore, the comparison of the H_2 production measured under radiolysis with the data obtained according to charge slippage[28] leads to the same ranking of electrochemical systems.

© 2022 The Authors. Small Methods published by Wiley-VCH GmbH

This result also indicates that the charge slippage of the batteries studied in detail by Dahn's group is strongly correlated to the stability of the considered electrolyte. Moreover, the production of H_2 appears as a good means to investigate the degradation of electrolyte in a cell when reduction processes are the major ones, such as on graphite and silicon electrodes.

It is known from previous studies that the H_2 production is strongly influenced by the water amount in the electrolyte.[40] Bernhard et al. have shown that for an 1 M LiTFSI in an EC/EMC electrolyte containing 4000 ppm of deliberately added water, the H_2 production increases during the first three cycles of a pristine graphite working-electrode and a metallic counter electrode. It increased to 4.7 μmol_{H2} from 0.1 μmol_{H2} with a similar cell and electrolyte containing less than 20 ppm of water.[40] In the study by Dahn and coworkers, the water amount corresponded to 1100 ppm of water by mass in the electrolyte.[28] At this water amount, H_2 is expected to be the main gas formed. Again, this accounts for the similar order obtained from radiolytic H_2 production and charge slippage data.[40] Noteworthily, our results were obtained within a few hours while Dahn and coworkers determined the average value of charge slippage from cycle 11 to 15 of a $LiCoO_2$/graphite pouch cell (Figure S1, Supporting Information). Lastly, an electrolyte that reduces the H_2 formation, as deduced from radiolysis experiments, will have a very positive impact on cycling in the presence of a high water amount.

All the previous observations tend then to prove that irradiation can be used as a predictive tool to screen the stability of batteries by a simple study of electrolyte behavior, and in particular, of H_2 production.

In addition to the additives studied by Dahn and coworkers,[28] we also investigated the behavior of another additive, namely EA. In LIBs, the high melting points of carbonates used in electrolytes lead to a strong decrease in battery performance at low temperatures. The presence of EA allows operating the batteries at very low temperatures (below −20 °C).[43] Such improvement in performance motivates our study of the behavior of the electrolyte in the presence of this additive under irradiation. With this additive, the H_2 radiolytic yield is very similar, although a little bit lower, to the value measured in the reference electrolyte (containing no additive) (Figure 2). Interestingly, experiments performed in $Li[Ni_{1-x-y}Co_xAl_y]O_2$/graphite-SiO pouch cells containing EC:EMC:DMC (dimethyl carbonate), without and with EA (5%) and in presence of $LiPF_6$, evidence that the gas after the cell formation is very similar in presence or absence of EA.[44] Another study performed on Nickel-Manganese-Cobalt NMC(111)/graphite pouch cells and LCO/graphite pouch cells has also shown that, in the presence of VC as an additive, the exchange of EC:EMC for EA significantly increases the gas production during the cell formation.[45] All these data imply that EA leads to a significant gas production, in perfect agreement with our results. While these results demonstrate that EA is not an effective additive for reducing electrolyte aging, they provide additional evidence of the power of our method for evaluating and classifying additives.

Despite the fact that the results obtained above clearly show that the H_2 radiolytic yield is an important criterion, the influence of other experimental parameters (such as the nature of the linear carbonate and the amount of water) should also be checked. In the following paragraphs we show that these parameters in fact do not change the ranking of the various electrolytes.

2.2. Influence of Different Parameters on the H_2 Production

2.2.1. Influence of the Nature of the Linear Carbonate on the H_2 Radiolytic Yield

In order to investigate the influence of the nature of the carbonate on the H_2 radiolytic yields, both ethyl methyl carbonate and diethyl carbonate (DEC) were studied in the presence of some additives (VC, FEC, VEC, or EA). It appears clearly from **Figure 3** that the trends observed for the evolution of the H_2 radiolytic yield were very similar for both linear carbonates considered. Of course, the dihydrogen yields were slightly increased when DEC was used instead of EMC, due to the presence of an additional -CH_2- group. The obtained results thus prove that the H_2 radiolytic yield evolution is due to the nature of the additive and not to that of the linear carbonate. Therefore, regardless of the nature of the linear carbonate, the H_2 radiolytic yield appears to be a good marker of the electrolyte degradation.

2.2.2. Influence of the Water Amount on the H_2 Radiolytic Yield

As mentioned before, in the study by Dahn and coworkers, the battery ranking determined by charge slippage was dominated by

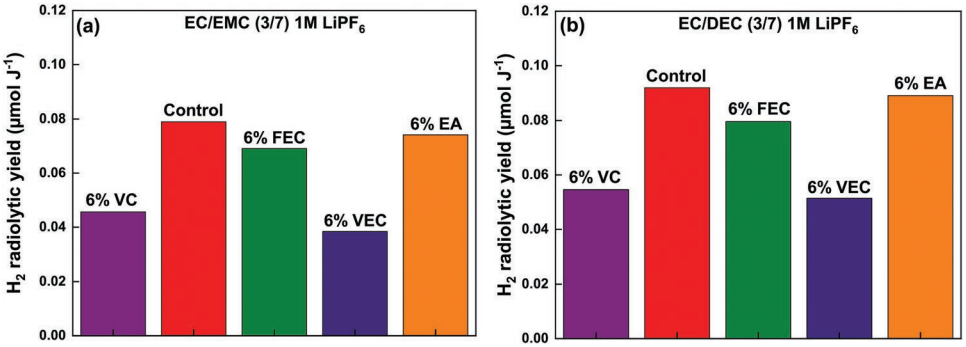


Figure 3. Evolution of the H_2 radiolytic yield for electrolytes containing a) EC/EMC (3/7 v/v) and b) EC/DEC (3/7 v/v) with 1 M $LiPF_6$ and various additives. The same color code as in Figure 2 is used. The uncertainty is estimated to be 7%.

© 2022 The Authors. Small Methods published by Wiley-VCH GmbH

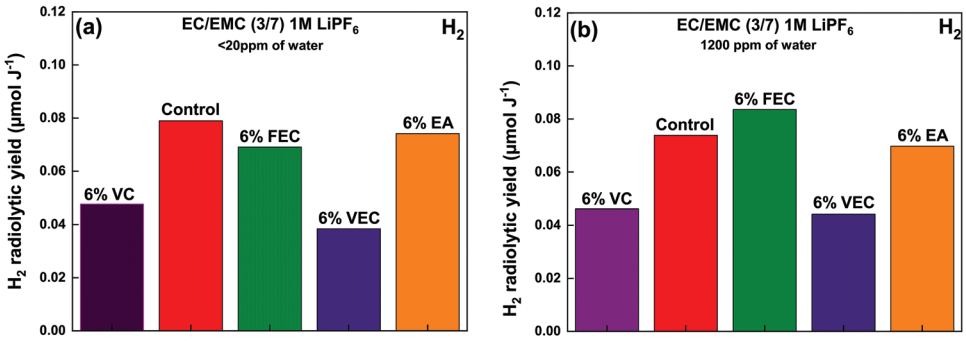


Figure 4. Evolution of the H_2 radiolytic yield for electrolytes EC/EMC (3/7 v/v) with 1 M $LiPF_6$ and various additives containing a) <20 ppm of water and b) 1200 ppm of water. The same color code as in Figure 2 is used. The uncertainty is estimated to be 7%.

H_2 gas production for electrolytes containing ≈1100 ppm of water by mass.[28] Therefore, in order to study the influence of the water amount on the H_2 radiolytic yield, water was deliberately added to the electrolyte to increase from 20–30 ppm to a value similar to 1100 (1200, here) ppm in the presence of the same additives as those studied above. It is clear from **Figure 4** that the trends observed for the evolution of the H_2 radiolytic yield as a function of the additive were similar at low or high water amounts, except for FEC. Indeed, when FEC was used, the H_2 radiolytic yield increased and even exceeded that of the reference sample. In fact, in this case, HF was produced in significant amounts due to the presence of a fluorine atom on the molecule (Figure 1).[37,46] It then reacted with the walls of the Pyrex glass ampoule. This reaction led in turn to the formation of water:

$$SiO_2 + 4HF \rightarrow SiF_4 + 2H_2O \quad (1)$$

Of course, this water formation will favor H_2 production. Thus, the higher H_2 radiolytic yield seen for FEC can be viewed as being partly due to the use of glass ampoules favoring water production. This was also experimentally confirmed. Indeed, after a dose of 25 kGy and for an initial water content of 1200 ppm, the water amount increased slightly to 1230 ppm in the reference sample while it went up to 1300 ppm when 6% of FEC was added in the electrolyte. The uncertainty of these titrations, based on 6 measurements, was estimated to be ≈2%. This can also account for the relatively high H_2 radiolytic yield measured previously in the sample containing FEC (Figure 2).

Therefore, the electrolyte ranking method proposed here is globally very robust, regardless of the water content in the electrolyte (from 20 to 1200 ppm). Furthermore, the above tests on the nature of the linear carbonate and the amount of water were performed quite rapidly and with minimal experimental uncertainty. This is in sharp contrast with electrochemical-based studies that could be envisaged.

2.3. Influence of the Presence of the Salt on the Gaseous Radiolytic Yields (total, H_2, and CO_2)

In order to obtain insights into reaction mechanisms, experiments were performed with and without the $LiPF_6$ salt and the radiolytic yields were compared in both cases (see **Figure 5**). The production of the total of the four gases of interest increased when the salt was added except in the case of FEC (Figure 5a). This global enhancement is clearly related to the strong CO_2 (Figure 5b) increase in the samples containing $LiPF_6$. By contrast, the CO and H_2 radiolytic yields decreased in the presence of the salt (see Figures S4a and S4b, Supporting Information), while the evolution of the methane radiolytic yield depended on the additive. Therefore, no trend appears clearly for this gas (Figure S4b, Supporting Information). Additionally, the order of the different electrolytes according to their H_2 radiolytic yield (Figure 5c) was similar in the presence or absence of $LiPF_6$ (with the exception of the sample containing FEC, see the comments in the preceding section).

For the purpose of comparison, the same gas measurements were performed in pure EMC and EC, respectively, with and without 1 M of $LiPF_6$ added. The corresponding radiolytic yield values are displayed in Table S1, Supporting Information. Clearly, $LiPF_6$ enhanced the total radiolytic yield, which is mainly due to a strong increase of the CO_2 yield. Similar to the observations performed on the reference electrolyte EC/EMC, the CO and H_2 radiolytic yields decreased in EMC and EC with 1 M $LiPF_6$ as compared to neat EMC and EC, while the CH_4 radiolytic yield increased. These effects will be discussed in detail in the "reaction mechanisms" section below.

2.4. Identification of Other Gases Produced upon Irradiation by Gas Chromatography coupled to Mass Spectrometry (GC-MS)

The knowledge of the various gases produced upon irradiation, in addition to H_2, CO, CO_2, and CH_4, is also important. Indeed, in LIBs, gas generation occurs simultaneously with SEI formation and arises from the decomposition of the electrolyte. Therefore, one way to check this decomposition is to identify the various gases produced to help determine the reaction mechanisms. In order to reach these goals, we firstly performed GC/MS experiments to identify the gas decomposition products formed upon irradiation.

An example of chromatogram presenting the peaks and their attribution obtained in the reference EC/EMC (3:7 v/v)/1 M $LiPF_6$ electrolyte irradiated at 6 kGy is shown in **Figure 6**. Besides the major gases already detected by µ-GC, alkanes (C_2H_6 and C_3H_8), a fluorinated alkane (C_2H_5F), an alkene (C_2H_4), dimethylether $(CH_3)_2O$, an acid (CH_3COOH) and an ester ($HCOOCH_3$) were also detected. In addition, we detected HF by means of nuclear magnetic resonance (NMR).

© 2022 The Authors. Small Methods published by Wiley-VCH GmbH

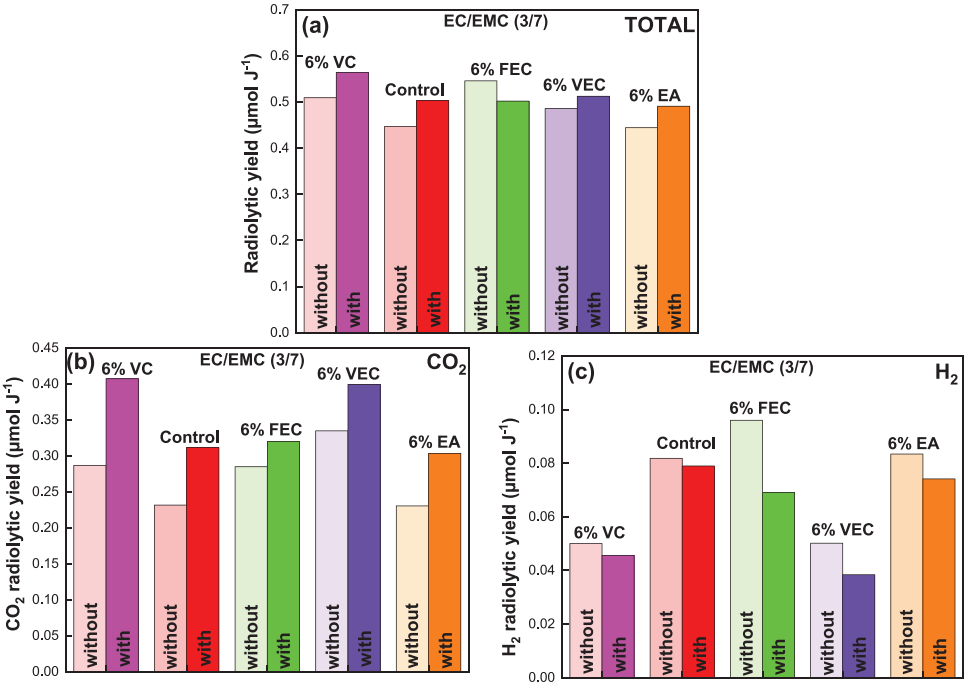


Figure 5. Evolution of radiolytic yields of a) the total of the four gases (CO_2, CO, H_2 and CH_4), b) CO_2, and c) H_2 gases produced after irradiation of electrolytes without or with $LiPF_6$ at 1 M. The uncertainty is estimated to be 7%.

The same experiments were performed for the various additives and at different irradiation doses. These measurements evidenced that the dose does not affect the nature of the formed gaseous products (see a typical example in Figure S5, Supporting Information). Conversely, the nature of the additive influenced the presence of the different gaseous species as summarized in Table S2, Supporting Information. In all cases, the following species were detected: CO_2, CO, H_2, CH_4, HF, C_2H_4, C_2H_5F, C_2H_6 and C_3H_8 (Figure 6 and Table S2, Supporting Information). Interestingly, all these gaseous species are generally observed in LIBs during the first charge or during cycling.[47,48] It should be noted that the origin of C_2H_4, CO, CH_4, and C_2H_6 produced during SEI formation is analyzed in details by isotope labeling in reference.[49] Table S2, Supporting Information, also shows that the nature of the additive has an impact on the formation of oxygenated molecules such as ethers, carboxylic acids, and esters. This suggests that the nature of the additive has an impact on reaction channels. Some species such as dimethyl ether, even methyl and ethyl ether, and methyl formate ($HCOOCH_3$) were identified in most samples after irradiation (Table S2, Supporting Information). Other species such as HCOOH, HO_2CCO_2H, $CH_3COOC_2H_5$, and CH_3COOH are more specific of the additive, which indicates that the presence of the additives induces preferential cleavages of some chemical bonds. Notably, the formation of ethers and of esters was also reported in GC/MS experiments performed on a EC/DMC/$LiPF_6$ electrolyte present in a cycled stainless steel/Li cell at 55 °C.[14]

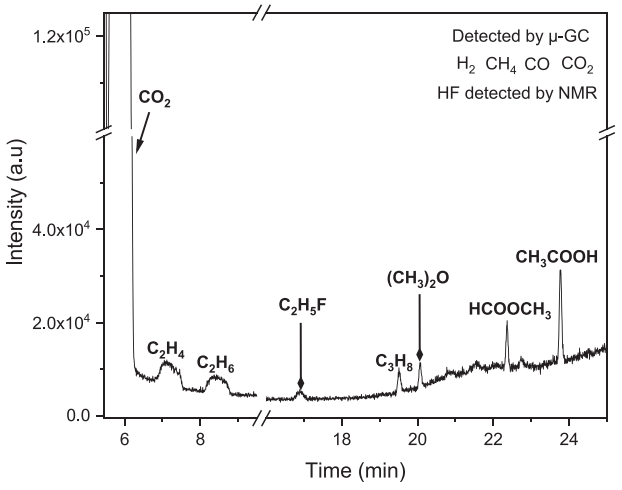


Figure 6. Gas decomposition products of the reference electrolyte (EC:EMC/1 M $LiPF_6$) were measured by GC/MS after a 6 kGy irradiation. The (H_2, CH_4, CO, CO_2) molecules written on the top, were identified and quantified by µ-GC experiments. HF was detected by NMR. CO_2 was identified by both µ-GC and GC/MS techniques. Other gases were identified by the GC/MS experiment only.

Other GC/MS experiments were performed on electrolytes irradiated at 100 kGy in order to obtain information about liquid phase degradation products. No clear feature of such degradation products was found, except in the case of the electrolyte containing 1 M $LiPF_6$ in EC/EMC (3/7 v/v) + 6% FEC (see Figure S6a, Supporting Information). An enlarged view of the chromatogram (Figures S6b,c, Supporting Information) shows that the amount of FEC decreased after a 100 kGy irradiation (see Figure S6b, Supporting Information) while VC is produced (Figure S6c, Supporting Information). This behavior was already observed after irradiation of neat FEC.[37] The formation of VC from FEC was also reported in the case of LIBs.

© 2022 The Authors. Small Methods published by Wiley-VCH GmbH

Thus, the reduction reaction of FEC to form LiF and VC, followed by subsequent VC reduction, was proposed.[50]

A full discussion on the effect of the presence an additive on the reaction channels is beyond the scope of the present work, but the production of the species common to all electrolytes and those found in the reference electrolyte is discussed below, with a focus on the H_2 production.

2.5. Reaction Mechanisms

The determination of reaction mechanisms is important to be able to control as much as possible the degradation of the electrolyte. For the sake of clarity, this section is focused on the reference electrolyte (1 M $LiPF_6$ in EC/EMC (3/7 v/v)) and on H_2 production due to its importance when reduction processes are considered. Additionally, since VC and VEC species decrease the H_2 radiolytic yield the most efficiently (**Figure 7**), a special focus will be made on these additives.

Upon irradiation, the primary effects of the ionizing radiation consist of the excitation and ionization of the molecule *M*:

$$M \rightarrow M^*, M^{\cdot+}, e^- \quad (2)$$

This is true also for a mixture where the fraction of the total absorbed energy transferred to each compound is proportional to the weight fraction of the compound and to the average mass collision stopping power of the compound for the various ionizing particles present in the medium. The latter term is generally assumed to be proportional to the *Z*/*A* ratios of the compounds, in which *Z* is the atomic number and *A* is the atomic mass number of the compound.[51]

Notably, linear (EMC) and cyclic (EC) carbonates behave markedly differently. While the electron gets solvated in the linear carbonate,[33,52] it attaches to the cyclic carbonate, leading to the formation of a radical anion ($EC^{\cdot-}$).[34–37] These very different behaviors can be rationalized thanks to DFT calculations, which show that in the gas phase, the first electron reduction for linear and cyclic carbonates is endothermic and exothermic, respectively.[53] In the EC:EMC mixture, the formed electron is surrounded both by EMC and EC molecules. In a previous picosecond pulse radiolysis experimental work performed on an EC/DEC (1/1) mixture, it was evidenced that once formed, the electron is very quickly trapped by EC molecules, which leads to the formation of $EC^{\cdot-}$ radical anions.[36] The signature of the solvated electron in DEC was not detected. This means that a formed electron can be very quickly trapped by EC molecules in contact of DEC molecules to form $EC^{\cdot-}$. The major channel for the formation of radical anions is thought to be the pre-solvated electron.[35,37] Of course, the same behavior can be expected in our reference electrolyte containing EC and EMC molecules.

Therefore, the $EC^{\cdot-}$ and $EC^{\cdot+}$ species are formed upon interaction between ionizing radiation and EC molecules. In previous work, we showed that CO and CO_2 could both be produced from the reductive and oxidative pathways generated from $EC^{\cdot-}$ and $EC^{\cdot+}$, respectively, in agreement with electrochemistry experiments.[36] In a very recent work, quantum chemistry calculations evidenced that EC molecules exist in solution as dimers and that radical cations are formed from these dimers, and not from a single molecule, implying that $EC^{\cdot+}$ should be more properly labeled as $EC_2^{\cdot+}$.[54] For the sake of clarity, we will rather write $EC^{\cdot+}$ below, even if the writing with the dimers should be more accurate. The ring of this radical cations opens, and the $^{\cdot}OCH_2CH_2OC^{\cdot+}O$ species is then formed. It leads to CO_2 production, and to a lesser extent, to CO.[55,56] This is consistent with DFT calculations which have evidenced that CO formation is more difficult than that of CO_2.[57,58] Concerning the fate of $EC^{\cdot-}$, it will mainly lead to CO, but also to CO_2 to a lesser extent.[56,59,60] In the case of EMC, only the fate of the $EMC^{\cdot+}$ radical cation has to be considered, as the electron has mostly attached to the EC molecule, as explained above. A reaction involving this radical cation is proposed in Figure 7. It is written consistently with that suggested in the case of irradiated DEC.[32]

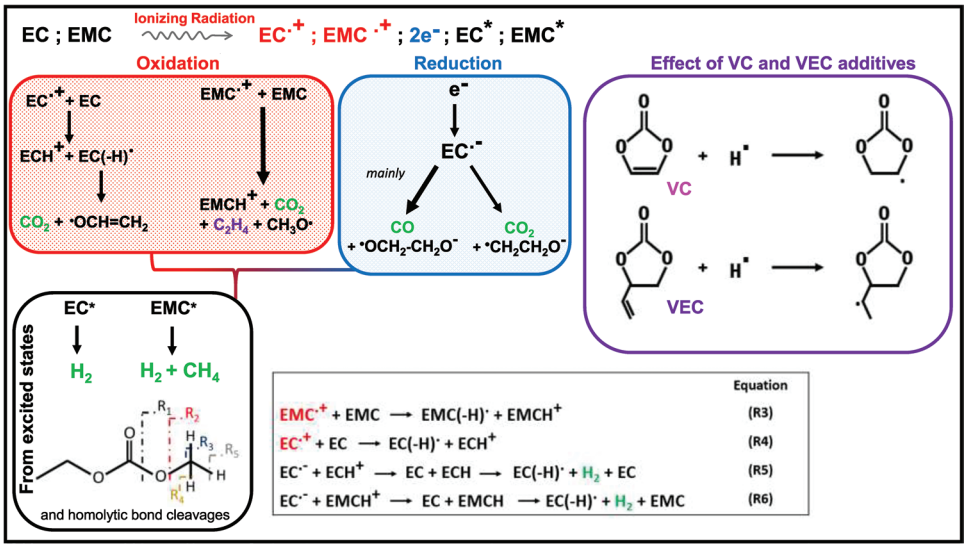


Figure 7. Proposed reactions taking place in the irradiated EC/EMC/1 M $LiPF_6$. Among the possible reaction pathways, oxidation of the carbonates is indicated in the red box and reduction is given in the blue box. The gases measured by gas chromatography μ-GC are indicated with a green color.

© 2022 The Authors. Small Methods published by Wiley-VCH GmbH

In irradiated neat solvents, the formation of H_2 was described as: i) arising from excited states and from the reaction of the solvated electron, yielding a $H^{\cdot}$ atom in both cases, that can dimerize to form H_2, when linear carbonates are considered[33]; ii) arising from species formed both from the reduction and oxidation channels in the case of cyclic carbonates.[34] Indeed, contrary to phenomena occurring in LIBs, both channels take place in the bulk of the irradiated solution. In the present case, as explained above, the formation of the electron solvated by EMC molecules is expected to be negligible as compared to the formation of an $EC^{\cdot -}$ radical anion. Therefore, processes leading to the formation of an H_2 molecule are mainly due to species arising both from the oxidation and reduction channels, as depicted by reactions (R5–R6) in Figure 7. Even if the reaction mechanisms are then different in radiolysis or in electrolysis, the effect of the additive, by scavenging more or fewer (or not) precursors of H_2, will lead to a similar ranking for both techniques. Of course, the values of H_2 production should be different in both techniques, but the evolution of this production remains the same.

Small molecules such as H_2 and CH_4 can be formed to a lower extent from the excited states, with H_2 arising from both EC* and EMC*, while methane can only be produced from EMC*.[36] However, the role of the EMC* excited states should be less important than in pure EMC due to an increased dielectric constant in the reference electrolyte as compared to pure EMC. Moreover, the reaction between the electron and the $EMC^{\cdot +}$ radical cation, giving rise to EMC*, will be less favored in the mixture than in neat EMC, due to very efficient electron attachment to the EC molecule. Homolytic bond cleavages also occur from excited states, leading to the release of radicals in the medium such as the $H^{\cdot}$ atom. Noteworthily, the $H^{\cdot}$ atom may also be produced by reactions channels such as after the reaction of the electron with protonated solvent molecules (ECH^+, $EMCH^+$). Once produced, the fate of these hydrogen atoms, and hence, of the H_2 molecule, will be affected by the presence of species that can scavenge them.

$LiPF_6$ also plays a crucial role in the reactions at stake, as increased CO_2 production is observed in the presence of the salt (Figure 5b). An emphasis on the role played by this salt is depicted in Figure S7, Supporting Information. It represents 12% of the mass of the reference electrolyte. The fraction of the total energy absorbed by the lithium hexafluorophosphate salt is also very close to 0.12. This direct interaction leads to reactions accounting for the formation of the PF_5 species, as well as of the fluorine atom and the fluoride anion (reactions R7-R10 in Figure S7, Supporting Information). In turn, PF_5 is responsible for the increased CO_2 production when the salt is added in the various electrolytes (Figure 5b). In EMC and EC, the CO_2 radiolytic yield increases from 0.18 and 0.29 to 0.25 and 0.43 μmol J^{-1}, respectively, when the $LiPF_6$ 1 M is added (Table S1, Supporting Information). This global increase in the presence of the salt can be rationalized as follows. PF_5 reacts readily with trace water molecules (reaction R11 in Figure S7, Supporting Information) and forms POF_3. This species reacts then with linear and cyclic carbonates to produce CO_2 in an autocatalytic manner (Figure S7, Supporting Information).[61] Moreover, recent ^{13}C-labeling of electrolytes have proposed a formation scheme for oligo-phosphate species which are produced in the liquid phase during the decomposition of the electrolyte.[17] Another work has also emphasized the role of the solvent cross-reactivity between linear and cyclic carbonates.[62] Of course, as $LiPF_6$ is present in the system and absorbs ionizing radiation, the CO and H_2 production arising from the carbonates present will logically decrease, as observed in Figures 5 and S4, Supporting Information.

The main reactions at stake in the reference electrolyte are depicted in Figures 7 and S7, Supporting Information. The reaction mechanism accounts for the various products detected in the gas phase. In Figure 7, besides the products detected by μ-GC (indicated with a green color) and C_2H_4, which was detected by GC/MS, formation of $^{\cdot}CH_3$ and $^{\cdot}OCH_3$ radicals will lead to the production of various compounds, such as C_2H_6, C_3H_8, and CH_3OCH_3, as detected by GC/MS (Figure 6). Note that $^{\cdot}CH_3$ radicals can also abstract $H^{\cdot}$ atoms from surrounding molecules to form CH_4.

Concerning the effect of additives, it is clear from Figure 2 that VC and VEC play an important role in decreasing the H_2 radiolytic yield, even if they are added at low amounts. We focus here on these two additives, as they exhibit the most contrasted behavior with respect to the reference electrolyte. In both cases, this lowest H_2 production can be attributed to the role of the double bond in the additive. It is indeed able to capture H_2 precursors, such as the hydrogen atom (Figure 7). The reaction of VC or VEC with the hydrogen atom leads to the formation of radical species that can then initiate the formation of polymers, among other compounds. The correlation between our results and those of Dahn and coworkers[28] suggests that the role of additives consists not only in improving the quality of the SEI, but also in decreasing the gas formation that leads to the formation of bubbles, which can for instance damage the contact between the electrodes and the SEI, or even the electrodes themselves.[63]

Thus, the various radiolysis experiments have enabled us not only to find a relevant criterion, based on the study by Dahn and coworkers,[28] for an efficient screening of LIB electrolytes, but also to propose reaction mechanisms taking place under irradiation. This enabled us to capture most of the behavior of the sample under aging. The study of Dahn and coworkers[28] was focused on reduction processes. Under other conditions, oxidation reactions with the formation of CO_2 may be the proper benchmark. For instance, a similar study to that presented here could be worth doing based on the recent publication on a battery using a positive electrode (NMC811), which is prone to intense reaction.[31] They are known to lead to CO_2 production.[64] Therefore, depending on the experimental conditions, the choice of the marker of the degradation in the radiation chemistry experiments, may be different.

Noteworthily, radiation chemistry can also be used to screen electrolytes in other systems of interest for energy storage, for examples post Li-ion devices such as sodium-ion batteries,[65,66] solid-state batteries[67] as well as supercapacitors.[68,69]

3. Conclusion

Radiolysis was shown to be an efficient tool for the fast screening of various electrolytes used in LIBs. The electrolytes

© 2022 The Authors. Small Methods published by Wiley-VCH GmbH

studied here were based on ethylene carbonate/ethyl methyl carbonate mixtures in the presence of a molar concentration of lithium hexafluorophosphate and various additives in different amounts. By analyzing the gaseous radiolytic products of these electrolytes, we obtained similar results to the work of J.R. Dahn and coworkers[28] after only a few hours of irradiation and with no manufacturing of or operating electrochemical cells. We evidenced that the measurement of the H_2 radiolytic yield is a relevant criterion to rank electrolytes and to compare with the foundational results of J.R. Dahn and coworkers.[28] Among all the systems studied, those containing vinylene carbonate or vinyl ethylene carbonate were shown to lead to the lowest dihydrogen radiolytic yields. This behavior was attributed to the presence of the carbon-carbon double bond able to scavenge precursors of the dihydrogen molecule. The conclusion of our work is that additives play an important role in LIBs, not only to improve the initial quality of the SEI, but also to decrease gas formation that can damage it over time. Our results were also found to be very robust towards various experimental conditions, such as the amount of water molecules and the nature of the linear carbonate. Reaction mechanisms, accounting for the formation of the major molecules in the electrolytes under irradiation, were also proposed.

Our results pave then the way to the use of radiation chemistry as a very efficient and robust technique for a first and quick screening of various electrolytes, in order to identify those which are potentially the most interesting ones. Of course, depending on the experimental conditions, i.e., whether oxidation or reduction processes are targeted, the nature of the gas used as a marker of the degradation processes will be different. Radiation chemistry is also applicable for the screening of systems other than LIBs, and will certainly be of great interest in the future to identify not only the best and most efficient electrolytes required for post-lithium-ion batteries, such as sodium-ion batteries, but also for supercapacitors and solid-state batteries.

4. Experimental Section

Chemicals and Sample Preparation: Anhydrous grade solutions of EC/EMC (3/7 v/v) mixed with 1 M $LiPF_6$ (>99.9%) were purchased from Mu Ionic solutions. Anhydrous grade EC, EMC, and DEC (purity of all > 99%) were obtained from Sigma-Aldrich. $LiPF_6$ was purchased from Solvionic (purity > 99.9%). The different additives used in this study are presented in Table S3, Supporting Information, together with the supplier and their purity. The corresponding chemical formulae are given in Figure 1.

The electrolytes were prepared in an argon-filled glove box (O_2 < 3 ppm and H_2O < 1 ppm). Water concentration, measured by a coulometric Karl-Fischer titration, was never higher than 30 ppm. For some experiments requiring more water, a very small quantity of high purity distilled water had been added to electrolytes (containing a small amount of water) to reach 1200 ppm of water and the final concentration was also checked by Karl Fischer titration.

The compounds were used without any further purification. A molecular sieve (3Å) was used to achieve less than 30 ppm of water in electrolytes when it was necessary. It was used before adding the lithium salt in the solvent.

The reference electrolyte used for these experiments was 1 M $LiPF_6$ in EC/EMC (3/7 v/v). The dielectric constant of this mixture was measured to be 18.5 at 298 K.[70]

For the radiolysis experiments, electrolytes were placed in a Pyrex glass ampoule. The samples were degassed during 30 min by argon bubbling. Afterward, they were outgassed at ≈1 mbar and subsequently filled with 1.5 bar of argon 6.0 (99.9999%). This operation was repeated three times.

Irradiation Experiments: A gamma irradiator Gammacell 3000 with a ^{137}Cs source was used. The dose rate (4.7 ± 0.2 Gy min^{-1}, with 1 Gray, denoted by Gy, equal to 1 J kg^{-1}) was measured using the Fricke dosimeter.[38] Each irradiation takes a few hours. Generally, a sample was irradiated four times successively. After each irradiation, gas measurements described above are carried out. Thus, it is possible to obtain results in just a few hours, after each irradiation step. In all irradiation experiments, and according to the stopping powers in the carbonates and in water, the dose received by the various electrolytes and by water was considered to be the same.

Gas Phase Analytical Methods: The degradation gases produced by irradiation were identified and quantified. The amount of H_2, CH_4, CO, and CO_2 gases was quantified by gas chromatography (μ-GC-R3000, SRA instrument) using ultra-high purity argon and helium as carrier gases.[71]

Moreover, in order to fully identify the degradation products formed in the gas phase, a Gas Chromatograph Agilent 6890 coupled with a mass spectrometer Agilent 5973 MS (GC/MS) was used. The mass spectrometer is equipped with an electron impact (EI) source, and a quadrupole mass analyzer. The mass range was 4–160. Helium was used as the vector gas with a flow rate of 2 mL min^{-1}. Separation was carried out by two distinct separation modes: on one hand, with a CP-PorabondQ (25 m, ∅ 0.32 mm) column (Varian), and on the other hand, with a two columns system connected in parallel, a molecular sieve Rt-MSieve 5 Å PLOT (30 m, ∅ 0.53 mm) column (Restek) and a Rt-Q-PLOT (30 m, ∅ 0.32 mm) column (Restek). The injector was set at 110 °C in splitless mode.

Supporting Information

Supporting Information is available from the Wiley Online Library or from the author.

Acknowledgements

Program Focus Batteries of CEA were gratefully acknowledged for financial support, as well as funding from the Agence Nationale de la Recherche (ANR ACETONE N° ANR-20-CE09-0010-01). Dr Magali Gauthier is gratefully acknowledged for fruitful discussions. The authors gratefully thank Dr Mark Levenstein for reading the manuscript, suggesting improvements, and making insightful comments.

Conflict of Interest

The authors declare no conflict of interest.

Data Availability Statement

The data that support the findings of this study are openly available in ZENODO at https://doi.org/10.5281/zenodo.6569796, reference number 6569796.

Keywords

aging, electrolytes, lithium-ion batteries, radiolysis, screening

Received: June 2, 2022
Revised: July 18, 2022
Published online:

© 2022 The Authors. Small Methods published by Wiley-VCH GmbH

[1] J. M. Tarascon, M. Armand, *Nature* **2001**, *414*, 359.
[2] D. Larcher, J. M. Tarascon, *Nat. Chem.* **2015**, *7*, 19.
[3] M. Winter, B. Barnett, K. Xu, *Chem. Rev.* **2018**, *118*, 11433.
[4] T. Kim, W. Song, D.-Y. Son, L. K. Ono, Y. Qi, *J. Mater. Chem. A* **2019**, *7*, 2942.
[5] Y. Wu, W. Wang, J. Ming, M. Li, L. Xie, X. He, J.-J. Wang, S. Liang, Y. Wu, *Adv. Funct. Mater.* **2019**, *29*, 1805978.
[6] R. Schmuch, R. H. Wagner, G. T. Placke, M. Winter, *Nat. Energy* **2018**, *3*, 267.
[7] A. Kwade, W. Haselrieder, R. Leithoff, A. Modlinger, F. Dietrich, K. Droeder, *Nat. Energy* **2018**, *3*, 290.
[8] M. R. Palacin, A. de Guibert, *Science* **2016**, *351*, 1253292.
[9] K. Xu, *Chem. Rev.* **2014**, *114*, 11503.
[10] J. Kalhoff, G. G. Eshetu, D. Bresser, S. Passerini, *ChemSusChem* **2015**, *8*, 2154.
[11] I. Cekic-Laskovic, N. von Aspern, L. Imholt, S. Kaymaksiz, K. Oldiges, B. R. Rad, M. Winter, in *Electrochemical Energy Storage: Next Generation Battery Concepts* (Ed.: R.-A. Eichel), Springer International Publishing, Cham **2019**, pp. 1–64.
[12] S. Laruelle, S. Pilard, P. Guenot, S. Grugeon, J. M. Tarascon, *J. Electrochem. Soc.* **2004**, *151*, A1202.
[13] G. Gachot, S. Grugeon, M. Armand, S. Pilard, P. Guenot, J.-M. Tarascon, S. Laruelle, *J. Power Sources* **2008**, *178*, 409.
[14] G. Gachot, P. Ribière, D. Mathiron, S. Grugeon, M. Armand, J.-B. Leriche, S. Pilard, S. Laruelle, *Anal. Chem.* **2011**, *83*, 478.
[15] J. Henschel, J. M. Dressler, M. Winter, S. Nowak, *Chem. Mater.* **2019**, *31*, 9970.
[16] J. Henschel, C. Peschel, F. Günter, G. Reinhart, M. Winter, S. Nowak, *Chem. Mater.* **2019**, *31*, 9977.
[17] J. Henschel, C. Peschel, S. Klein, F. Horsthemke, M. Winter, S. Nowak, *Angew. Chem., Int. Ed.* **2020**, *59*, 6128.
[18] K. Xu, *Chem. Rev.* **2004**, *104*, 4303.
[19] S. Chattopadhyay, A. L. Lipson, H. J. Karmel, J. D. Emery, T. T. Fister, P. A. Fenter, M. C. Hersam, M. J. Bedzyk, *Chem. Mater.* **2012**, *24*, 3038.
[20] F. Lindgren, C. Xu, L. Niedzicki, M. Marcinek, T. Gustafsson, F. Björefors, K. Edström, R. Younesi, *ACS Appl. Mater. Interfaces* **2016**, *8*, 15758.
[21] L. Seidl, S. Martens, J. Ma, U. Stimming, O. Schneider, *Nanoscale* **2016**, *8*, 14004.
[22] A. Wang, S. Kadam, H. Li, S. Shi, Y. Qi, *npj Comput. Mater.* **2018**, *4*, 15.
[23] A. M. Haregewoin, A. S. Wotango, B.-J. Hwang, *Energy Environ. Sci.* **2016**, *9*, 1955.
[24] M. D. Halls, K. Tasaki, *J. Power Sources* **2010**, *195*, 1472.
[25] O. Borodin, M. Olguin, C. E. Spear, K. W. Leiter, J. Krap, *Nanotechnology* **2015**, *26*, 354003.
[26] S. Brox, S. Röser, T. Husch, S. Hildebrand, O. Fromm, M. Korth, M. Winter, I. Cekic-Laskovic, *ChemSusChem* **2016**, *9*, 1704.
[27] A. D. Sendek, Q. Yang, E. D. Cubuk, K.-A. N. Duerloo, Y. Cui, E. J. Reed, *Energy Environ. Sci.* **2017**, *10*, 306.
[28] D. Y. Wang, N. N. Sinha, R. Petibon, J. C. Burns, J. R. Dahn, *J. Power Sources* **2014**, *251*, 311.
[29] F. Horsthenke, A. Friesen, X. Mönnighoff, Y. P. Stenzel, M. Grützke, J. T. Andersson, M. Winter, S. Nowak, *RSC Adv.* **2017**, *7*, 46989.
[30] F. Hildenbrand, F. Aupperle, G. Stahl, E. Figgmeier, D. U. Sauer, *Batteries Supercaps* 202200038.
[31] W. Song, J. Harlow, E. Logan, H. Hebecker, M. Coon, L. Molino, M. Johnson, J. Dahn, M. Metzger, *J. Electrochem. Soc.* **2021**, *168*, 090503.
[32] D. Ortiz, V. Steinmetz, D. Durand, S. Legand, V. Dauvois, P. Maître, S. L. Caër, *Nat. Commun.* **2015**, *6*, 6950.
[33] D. Ortiz, I. Jimenez Gordon, J.-P. Baltaze, O. Hernandez-Alba, S. Legand, V. Dauvois, G. Si Larbi, U. Schmidhammer, J. L. Marignier, J.-F. Martin, J. Belloni, M. Mostafavi, S. Le Caër, *ChemSusChem* **2015**, *8*, 3605.
[34] D. Ortiz, I. Jimenez Gordon, S. Legand, V. Dauvois, J.-P. Baltaze, J. L. Marignier, J.-F. Martin, J. Belloni, M. Mostafavi, S. Le Caër, *J. Power Sources* **2016**, *326*, 285.
[35] S. L.e Caër, D. Ortiz, J. L. Marignier, U. Schmidhammer, J. Belloni, M. Mostafavi, *J. Phys. Chem. Lett.* **2016**, *7*, 186.
[36] F. Wang, F. Varenne, D. Ortiz, V. Pinzio, M. Mostafavi, S. L.e Caër, *ChemPhysChem* **2017**, *18*, 2799.
[37] M. Puget, V. Shcherbakov, S. Denisov, P. Moreau, J.-P. Dognon, M. Mostafavi, S. L. Caër, *Chem. - Eur. J.* **2021**, *27*, 8185.
[38] H. Fricke, E. J. Hart, in *Radiation Dosimetry*, Second Edition ed. (Eds.: F. H. Attix, W. C. Roesch), Academic press, New York and London **1966**, *Vol. 2*, pp. 167-232.
[39] H. Yoshida, T. Fukunaga, T. Hazama, M. Terasaki, M. Mizutani, M. Yamachi, *J. Power Sources* **1997**, *68*, 311.
[40] R. Bernhard, M. Metzger, H. A. Gasteiger, *J. Electrochem. Soc.* **2015**, *162*, A1984.
[41] M. Metzger, B. Strehle, S. Solchenbach, H. A. Gasteiger, *J. Electrochem. Soc.* **2016**, *163*, A798.
[42] S. S. Zhang, *J. Power Sources* **2006**, *162*, 1379.
[43] S. Herreyre, O. Huchet, S. Barusseau, F. Perton, J. M. Bodet, P. Biensan, *J. Power Sources* **2001**, *97*, 576.
[44] X. Ma, R. S. Arumugam, L. Ma, E. Logan, E. Tonita, J. Xia, R. Petibon, S. Kohn, J. R. Dahn, *J. Electrochem. Soc.* **2017**, *164*, A3556.
[45] R. Petibon, J. Harlow, D. B. Le, J. R. Dahn, *Electrochim. Acta* **2015**, *154*, 227.
[46] K. Kim, I. Park, S.-Y. Ha, Y. Kim, M.-H. Woo, M.-H. Jeong, W. C. Shin, M. Ue, S. Y. Hong, N.-S. Choi, *Electrochim. Acta* **2017**, *225*, 358.
[47] J. Wen, Y. Yu, C. Chen, *Mater. Express* **2012**, *2*, 197.
[48] Y. P. Stenzel, F. Horsthemke, M. Winter, S. Nowak, *Separations* **2019**, *6*, 26.
[49] M. Leißing, C. Peschel, F. Horsthemke, S. Wiemers-Meyer, M. Winter, S. Nowak, *Batteries Supercaps* **2021**, *4*, 1731.
[50] A. L. Michan, B. S. Parimalamn, M. Leskes, R. N. Kerber, T. Yoon, C. P. Grey, B. L. Lucht, *Chem. Mater.* **2016**, *28*, 8149.
[51] J. W. T. Spinks, R. J. Woods, *An Introduction to Radiation Chemistry*, 3rd ed., Wiley-Interscience Publication, New York, USA **1990**.
[52] F. Torche, A. K. El Omar, P. Babilotte, S. Sorgues, U. Schmidhammer, J.-L. Marignier, M. Mostafavi, J. Belloni, *J. Phys. Chem. A* **2013**, *117*, 10801.
[53] K. Tasaki, *J. Phys. Chem. B* **2005**, *109*, 2920.
[54] I. V. Beregovaya, I. S. Tretyakova, V. I. Borovkov, *J. Phys. Chem. Lett.* **2021**, *12*, 11573.
[55] M. Metzger, J. Sicklinger, D. Haering, C. Kavakli, C. Stinner, C. Marino, H. A. Gasteiger, *J. Electrochem. Soc.* **2015**, *162*, A1227.
[56] K. N. Shitaw, S.-C. Yang, S.-K. Jiang, C.-J. Huang, N. A. Sahalie, Y. Nikodimos, H. H. Weldeyohannes, C.-H. Wang, S.-H. Wu, W.-N. Su, B. J. Hwang, *Adv. Funct. Mater.* **2021**, *31*, 2006951.
[57] L. Xing, W. Li, C. Wang, F. Gu, M. Xu, C. Tan, J. Yi, *J. Phys. Chem. B* **2009**, *113*, 16596.
[58] J. L. Tebbe, T. F. Fuerst, C. B. Musgrave, *ACS Appl. Mater. Interfaces* **2016**, *8*, 26664.
[59] I. A. Shkrob, Y. Zhu, T. W. Marin, D. Abraham, *J. Phys. Chem. C* **2013**, *117*, 19255.
[60] B. B. Berkes, A. Schiele, H. Sommer, T. Brezesinski, J. Janek, *J. Solid State Electrochem.* **2016**, *20*, 2961.
[61] C. L. Campion, W. T. Li, B. L. Lucht, *J. Electrochem. Soc.* **2005**, *152*, A2327.
[62] C. Peschel, F. Horsthemke, M. Leißing, S. Wiemers-Meyer, J. Henschel, M. Winter, S. Nowak, *Batteries Supercaps* **2020**, *3*, 1183.
[63] K. Kim, H. Ma, S. Park, N.-S. Choi, *ACS Energy Lett.* **2020**, *5*, 1537.
[64] B. Rowden, N. Garcia-Araez, *Energy Rep.* **2020**, *6*, 10.
[65] A. Ponrouch, D. Monti, A. Boschin, B. Steen, P. Johansson, M. R. Palacín, *J. Mater. Chem. A* **2015**, *3*, 22.
[66] H. Hijazi, P. Desai, S. Mariyappan, *Batteries Supercaps* **2021**, *4*, 881.
[67] K. H. Park, Q. Bai, D. H. Kim, D. Y. Oh, Y. Zhu, Y. Mo, Y. S. Jung, *Adv. Energy Mater.* **2018**, *8*, 1800035.
[68] W. Ye, H. Wang, J. Ning, Y. Zhong, Y. Hu, *J. Energy Chem.* **2021**, *57*, 219.
[69] A. Balducci, *J. Power Sources* **2016**, *326*, 534.
[70] D. S. Hall, J. Self, J. R. Dahn, *J. Phys. Chem. C* **2015**, *119*, 22322.
[71] C. Fourdrin, H. Aarrachi, C. Latrille, S. Esnouf, F. Bergaya, S. L.e Caër, *Environ. Sci. Technol.* **2013**, *47*, 9530.

© 2022 The Authors. Small Methods published by Wiley-VCH GmbH